RSC Advances

This is an *Accepted Manuscript*, which has been through the Royal Society of Chemistry peer review process and has been accepted for publication.

Accepted Manuscripts are published online shortly after acceptance, before technical editing, formatting and proof reading. Using this free service, authors can make their results available to the community, in citable form, before we publish the edited article. This *Accepted Manuscript* will be replaced by the edited, formatted and paginated article as soon as this is available.

You can find more information about *Accepted Manuscripts* in the Information for Authors.

Please note that technical editing may introduce minor changes to the text and/or graphics, which may alter content. The journal's standard Terms & Conditions and the Ethical guidelines still apply. In no event shall the Royal Society of Chemistry be held responsible for any errors or omissions in this *Accepted Manuscript* or any consequences arising from the use of any information it contains.

ROYAL SOCIETY OF CHEMISTRY

www.rsc.org/advances

Silk/Chitosan Biohybrid Hydrogels and Scaffolds via Green Technology

Sangram K.Samal[1,2,3], Mamoni Dash[1,4], Federica Chiellini[1], Xiaoqin Wang[2], Emo Chiellini[1], Heidi A. Declercq[5] and David L. Kaplan[2]

1. BioLab- UdR-INSTM, Via Vecchia Livornese, University of Pisa, Pisa - 1291, Italy
2. Department of Biomedical Engineering, 4 Colby Street, Tufts University, Medford, MA 02155, United States
3. Laboratory of General Biochemistry and Physical Pharmacy, Center for Nano- and Biophotonics, Gent University, Ottergemsesteenweg 460, B-9000 Gent, Belgium.
4. Polymer Chemistry & Biomaterials Research Group, Ghent University, Krijgslaan 281, S4-Bis, B-9000 Ghent, Belgium
5. Department of Basic Medical Sciences – Tissue Engineering Group, Ghent University, De Pintelaan 185 (6B3), 9000 Ghent, Belgium.

RSC Advances Accepted Manuscript

ABSTRACT

Silk fibroin protein-based hydrogels and 3D scaffolds in combinations with chitosan were designed with a focus on green technology. Physico-chemical properties were modulated using ultrasonication processing to avoid the use of organic solvents or chemical crosslinking. The ultrasonication of mixtures of silk and chitosan induced a conformational change of silk from random coil to β-sheet resulting in the self-assembly of the hydrophobic peptide segments in the protein, entrapping chitosan chains in these silk networks. These biohybrid materials were prepared with different physico-chemical properties by varying the relative concentrations of silk and chitosan. In combination with lyophilization, interconnected porous 3D scaffolds with controlled morphologies were generated. MC3T3-E1 cells were successfully encapsulated in silk fibroin protein and silk fibroin protein- chitosan hydrogels and colonized the scaffolds. These engineered biohybrid hydrogel network systems can also be utilized to encapsulate bioactive molecules, thus

providing a versatile set of biomaterials with retention of degradability, but without the use of organic solvents or chemical crosslinking during preparation.

Key words – silk fibroin protein, chitosan, ultrasonication, biohybrid, biomaterials

1. Introduction

Natural polymers have inherent biological recognition properties and are often considered useful biomaterials for therapeutic applications.[1, 2] Silk fibroin protein derived from *Bombyx mori* cocoons is a promising natural protein polymer that has been widely studied due to its unusual amino acid composition and chemistry and widely used for biomedical and other applications.[3] Silk has a unique combination of blood compatibility, wet state mechanical strength, cell biocompatibility, water-vapor permeability in film form, and can be modified chemically or physically to alter properties and to immobilize biomolecules.[4-6] Silk 3D scaffold materials have been employed in tissue engineering in combination with mesenchymal stem cells, endothelial cells and co-cultures of mature endothelial cells and primary osteoblasts.[7-10] Silk based-biomaterials have also achieved FDA approval for some biomedical applications.[11, 12]

Silk forms semicrystalline protein materials, with the protein primarily composed of repetitive sequences of the amino acids: glycine, alanine serine and tyrosine.[13] The molecular conformation of silk is an important parameter to control, since this affects the physical properties of materials formed from the protein. Silk secondary structures, silk I and silk II[14] , include the metastable silk I and the stable silk II which consists of anti-parallel β-sheets and confers insolubility in water.[15] Silk biomaterials can be transformed to insoluble materials by changing the conformation from silk I to silk II through physical or chemical treatments, such as high temperature, high humidity, immersion in some organic solvents or the input of energy such as via sonication or vortexing.[2, 11, 16, 17] However, silk materials can be brittle in the dry state, depending on the processing method utilized,

RSC Advances Accepted Manuscript

limiting some utility unless properly annealed in water vapor or processed with plasticizers such as glycerol.

For long-term biomedical applications, the stability and mechanical properties of hydrogels require control of properties. Therefore combinations of polysaccharides with silk can provide new options for modulation of such properties. Chitosan is a naturally derived cationic polysaccharide composed of randomly distributed N-acetyl glucosamine and D-glucosamine sugars. The polymer exhibits three reactive sites for modification, a primary amine and two primary or secondary hydroxyl groups per glucosamine unit.[18, 19] The structural characteristics of chitosan mimic glycosaminoglycan components of the extracellular matrix, while the biocompatibility, biodegradability, antibacterial, antioxidant activity and mucoadhesive properties impart versatility. The utilization of chitosan in biomedical applications is limited in part due to its low solubility at physiological pH, inferior mechanical properties and high swelling ability.[18, 20-22] In order to overcome these limitations, chitosan has been conjugated or blended with silk fibroin protein. The combination of these two biopolymers silk fibroin protein and chitosan improved physico-chemical properties and mimic the naturally occurring environment of certain tissues.[23-25]

An important feature of silk and chitosan are the polymer charge states at neutral pH, with silk having a net negative charge in contrast to the positive charged primary amine groups of chitosan. These charges can be exploited to generate electrostatic complexes as we have utilized in our prior studies with elastin-silk protein alloys.[26] In these all protein alloys, electrostatic mechanisms were used to modulate the material properties.

There are many studies on silk and chitosan biomaterials attained through blends or crosslinked conjugates.[24, 27, 28] However, usually organic solvents are employed during the fabrication process. In certain cases where biomaterials were used to encapsulate labile drugs or bioactive compounds, denaturation of the drug can occur due to these organic solvents.[29, 30] Traces of organic solvents or acids in biomaterials can also be problematic and lead to loss of biocompatibility.[31-33] Therefore,

RSC Advances Accepted Manuscript

more biocompatible systems without the need for chemical reagents to fabricate silk/chitosan conjugate biomaterials would provide new options for utility of these blends. The most commonly used green technologies in biomaterials fabrication processes are water, ultrasonication, supercritical carbon dioxide and ionic liquids. In this context, ultrasonication is promising to control polymer features,[34-36] while not altering the chemical nature of the polymers.[37] Despite several studies on biohybrid silk/chitosan systems using solvents and chemical crosslinking strategies, the utilization of ultrasound in processing has not been reported.

In the present research, a green technique based on ultrasonication was employed to generate and control the properties of silk/chitosan mixtures, forming interpenetrating networks for hydrogels. Silk/chitosan 3D porous scaffolds were obtained by lyophilizing the hydrogels. The effects of chitosan ratio on silk/chitosan hydrogels and scaffold properties were studied, including stability, morphology, mechanical properties and cell compatibility.

2. Results and Discussion

2.1 Scanning electron microscopy (SEM)

Scaffold morphology and architecture impact cell interactions, including attachment, spreading and survival. SEM analysis was performed to examine the morphology and internal microarchitectures of the porous scaffolds (Figure 1). The SISF scaffolds showed porous structures with the presence of layers (Figure 1a & b). The SEM images of sonication induced silk/chitosan scaffolds are shown in Figure 1c-h. The scaffolds with low content of chitosan (SC1 scaffold) showed well organized porous interconnected structures, while increasing the chitosan content generated spongy scaffolds with flower-like structures. The sonication induced silk/chitosan scaffolds were highly porous, which should aid in the infiltration and migration of cells or mass exchange (nutrition, oxygen and metabolic waste). The high porosity combined with interconnected porous structure make silk/chitosan scaffolds a useful structured biomaterial for tissue engineering needs.

RSC Advances Accepted Manuscript

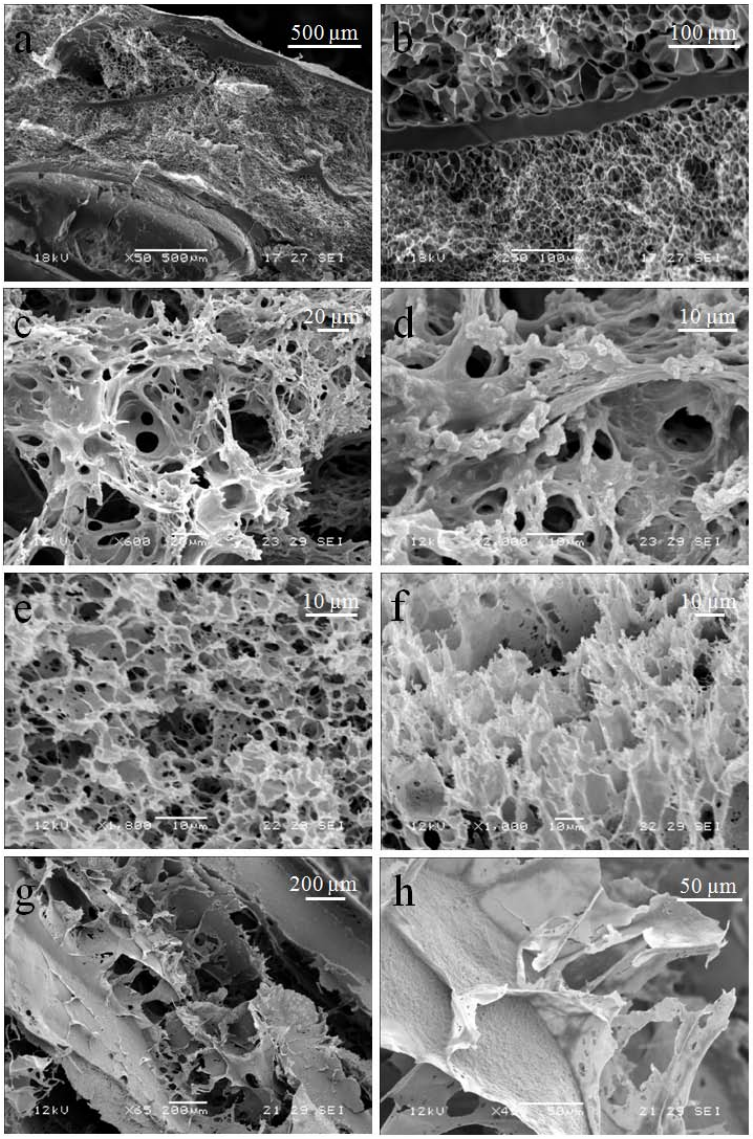

Figure 1. Morphologies of sonication induced (a & b) silk scaffold (SISF), (c & d) silk scaffold with 10% of chitosan (SC1), (e & f) silk scaffold with 25% of chitosan (SC2) and (g & h) silk scaffold with 50% of chitosan (SC3) were observed by SEM at (a, c, e & g) lower and (b, d, f & h) higher magnifications, respectively.

RSC Advances Accepted Manuscript

2.2 Wide angle X-ray scattering (WAXS)

The WAXS diffraction patterns of SISF, SC1, SC2 and SC3 images are shown in Figure 2. The addition of chitosan had a minimal effect on the crystallinity of silk. The crystalline structure of silk/chitosan scaffolds showed four distinct peaks between 5° and 35°. The diffraction peak around at 9°, 20° denoted random coil conformation, and around 24° denoted β-sheet structure of silk. The characteristic semi-crystalline structure of chitosan diffraction peaks generally appeared around at 11° and 20°.[38] The silk peaks dominated over chitosan in determining the crystalline structure of the silk/chitosan scaffolds as diffraction peaks associated with silk were the only peaks visible.

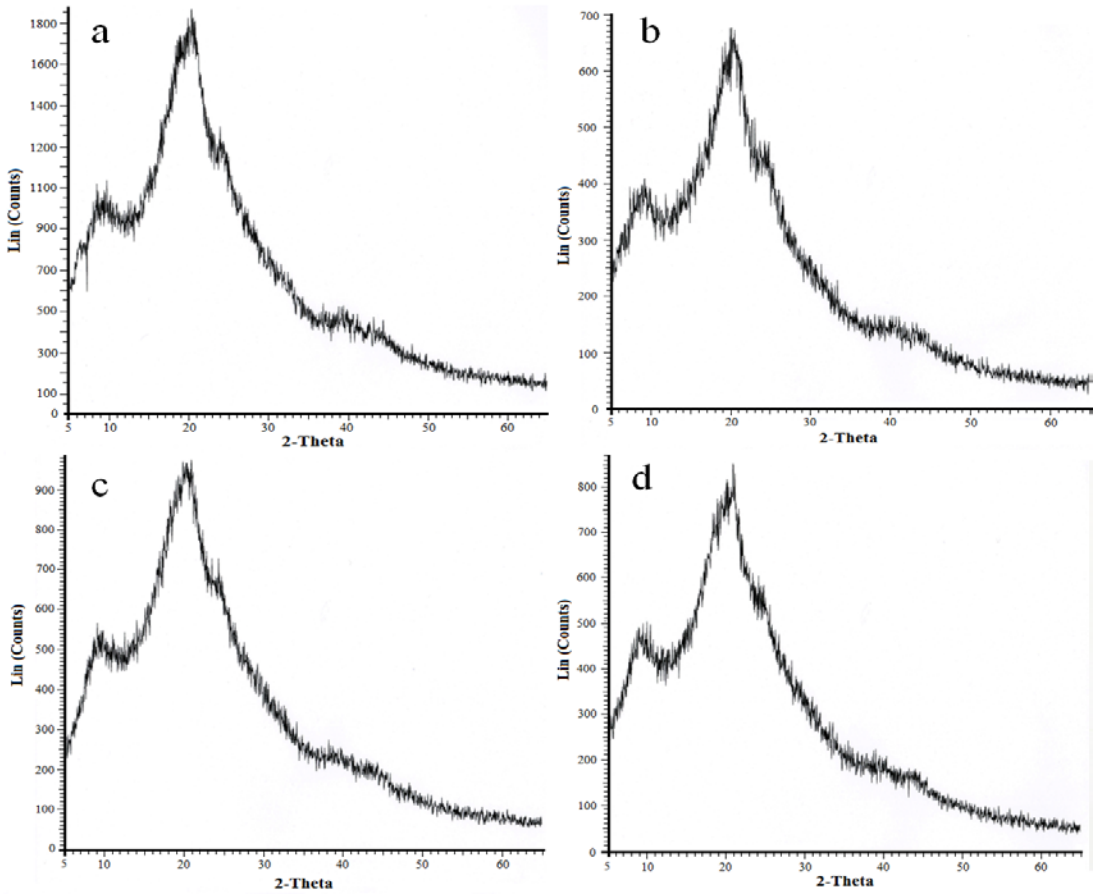

Figure 2. AXS diffraction patterns of (a) SISF, (b) SC1, (c) SC2 and (d) SC3 obtained by Kristalloflex 810 diffractometer using a Cu Kα (λ=1.5406 Å) as X-ray source. Scans were run in the high angle region 5° < 2θ < 65° at scan rate of 0.040°/min and a dwell time of 2s.

RSC Advances Accepted Manuscript

2.3 Mechanical analysis

The scaffolds should possess appropriate mechanical strength and elastic modulus in order to retain shape, pores and internal architecture for physical support for tissue development. Figure 3 provides yield strength and modulus, which indicate that at lower concentrations of chitosan increases in yield strength result, while increasing chitosan concentration decreased the yield strength of the silk/chitosan hydrogels. The modulus of the hydrogels also increased with lower concentrations of chitosan and decreased with further increases in the chitosan concentration.

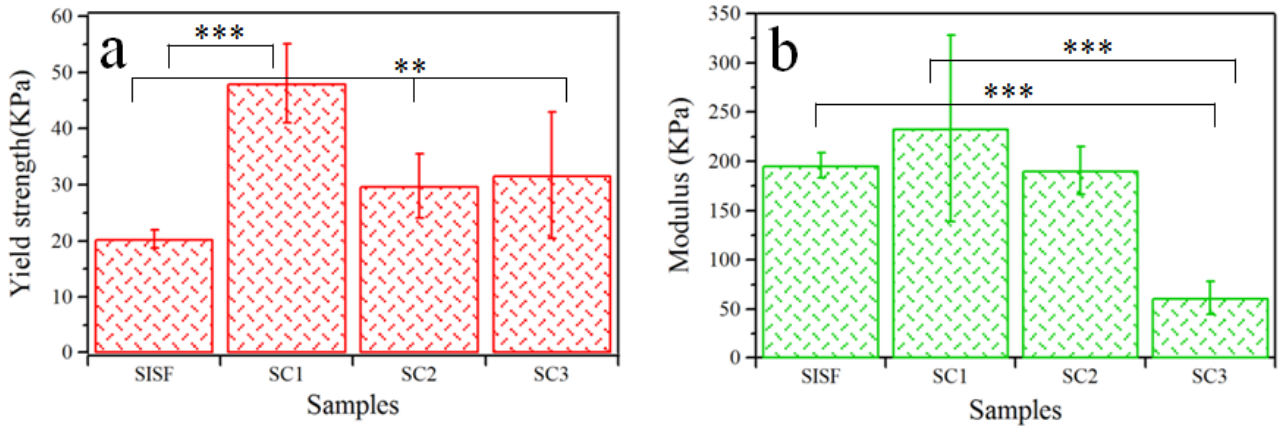

Figure 3. Mechanical properties - sonication induced SISF and silk/chitosan gels (a) yield strength (b) modulus, ** when significantly P<0.01 and *** when P<0.001.

2.4 Deswelling kinetics

The deswelling kinetics of ultrasound sonication induced silk/chitosan hydrogels provided information about the movement of water. The deswelling profiles of the silk/chitosan gels were recorded isothermally at 37°C during 180 minutes and weight loss data are shown in Table 1 and Figure 4.

RSC Advances Accepted Manuscript

Table 1. Deswelling weight loss of sonication induced hydrogels by TGA isothermal analysis.

Sample	0 – 30 min*	30 – 60 min*	60 – 90 min*	90 – 180 min*
SISF	54.7	22.3	12.7	10.1
SC1	43.5	12.9	11.9	11.8
SC2	54.1	20.7	8.9	7.3
SC3	57.4	25.4	6.4	4.7

*all values are in (wt. %)

The lower the amount of chitosan content in the samples showed faster deswelling behaviour compared to SISF, which is in contrast to the behaviour of the SC3 gel.

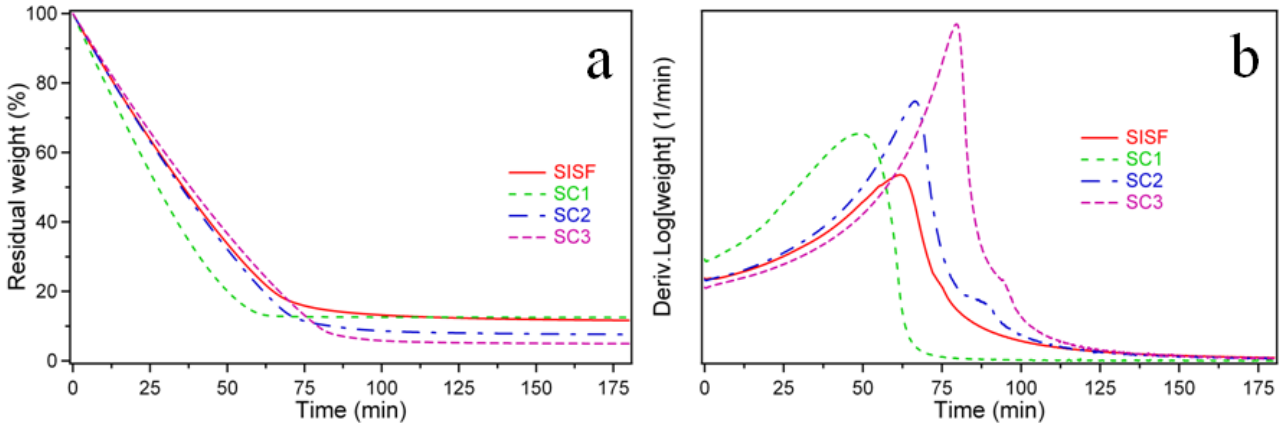

Figure 4. Deswelling kinetics spectra of (a) weight % and (b) derivative weight by water weight loss over time isothermally at 37°C to the dried state over time 180 min under a nitrogen atmosphere at a flow rate of 60 mL·min^{-1}by TGA, TA Q500-thermobalance.

Figure 4 shows the relative weight loss of SISF and silk/chitosan during 180 min of isothermal treatment at 37°C. The SC1 released more water within the first 60 min than SISF and the other silk/chitosan hydrogels. The deswelling behavior was significantly affected by the structural difference in SC1 in comparison with SISF and the other silk/chitosan hydrogels. After 100 min SISF and SC1 showed similar patterns of deswelling until 180 min. The SC2 and SC3 samples

RSC Advances Accepted Manuscript

released more water after 60 min. The spectra at 180 min showed that SC3 released more water compared to SC2, SC1 and SISF. The differences in deswelling kinetics are likely due to the structural and net charge differences of the samples.

2.5 State of water

Research on polymeric devices in the biomedical or pharmaceutical industries depends significantly on how water molecules associate. DSC analysis was employed to assess the type of water present in the different polymers. Free water freezes at the same temperature as pure water, whereas bound water does not freeze even at a very low temperature, due to its strong interaction with the polymer matrix.[3, 39] According to this hypothesis, the endotherm measured when warming the frozen gel represents the melting of free water, and this value will yield the amount of free water present in the hydrogel. The state of water and structural changes of water absorbed in ultrasound sonicated silk/chitosan were studied by DSC (Table 2).

Table 2. The state of water based on DSC.

Sample	W_t(%-wt)	W_f(%-wt)	W_{nf}(%-wt)
SISF	91.3±3.9	80.9±10.3	10.5±6.4
SC1	82.8±12.6	68.6±5.5	14.2±12.1
SC2	91.6±3.7	79.7±5.1	11.9±1.4
SC3	94.4±9.1	82.6±13.5	11.9±15.6

Total water (Wt), free water (Wf) and non-free water (Wnf) contents are reported in Fig. 5. The Wt and Wf values of SC1 were lower than that of SISF. The Wnf values of SC1, SC2 and SC3 were higher than SISF, attributed to increasing hydrophilic moiety upon addition of chitosan. The Wt and Wf contents were higher in SC3 than SIFP, SC1 and SC2.

RSC Advances Accepted Manuscript

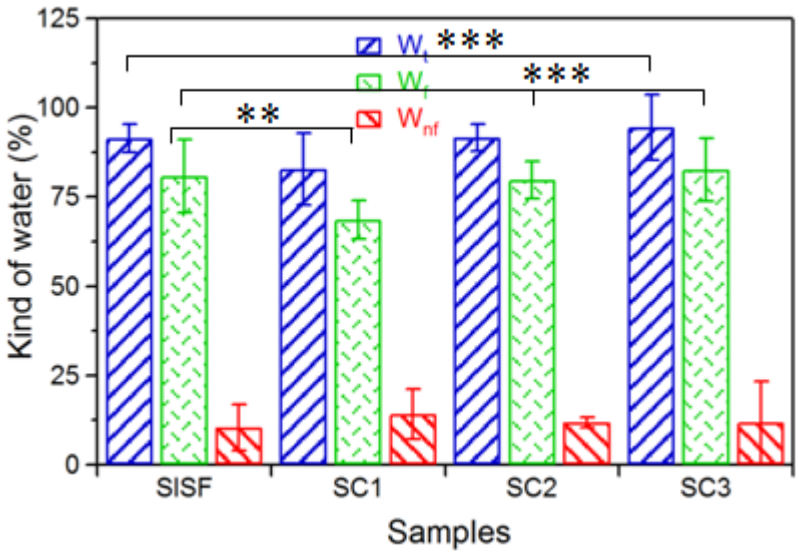

Figure 5. State of water of sonication induced SISF and silk/chitosan gels, where Wt = total water, Wf = free water and Wnf = non-free water significantly, ** when significantly P<0.01 and *** when P<0.001.

2.6 Attenuated total reflectance FTIR (ATR-FTIR)

ATR-FTIR was used to observe the structural properties of the ultrasound sonicated silk/chitosan hydrogels (Fig. 6). The silk/chitosan scaffold spectra were partly overlapped by those of SISF, with some band shifting. The general characteristic absorption bands of the silk random coil appears at 1660 cm^{-1} for amide-I, 1540 cm^{-1} for amide-II and 1235 cm^{-1} for amide-III. Absorption bands for the sonicated silk and silk/chitosan hydrogels were at 1635 cm^{-1} for amide-I, 1530 cm^{-1} for amide-II and 1240 cm^{-1} for amide-III, which were attributed to structural changes in silk into β-sheet conformation, with some random coil.

RSC Advances Accepted Manuscript

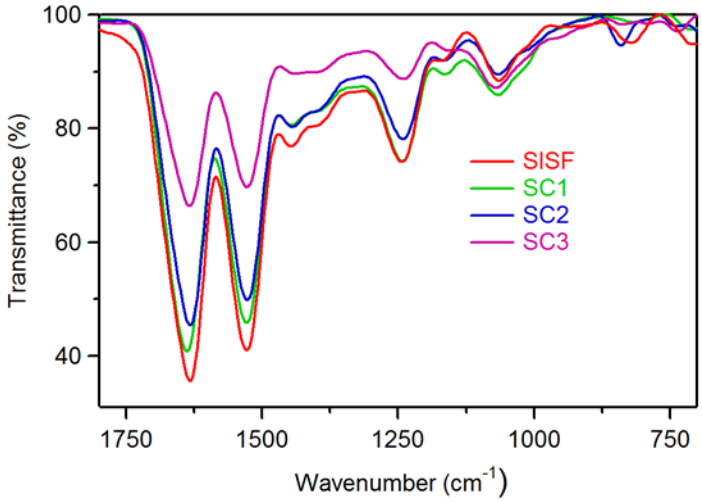

Figure 6. ATR-FTIR spectra of SISF/chitosan scanned over the range 2000–700 cm^{-1}.

The results suggest that ultrasonication induced a change in silk structure due to the self-assembly of the crystalline hydrophobic domains, as we have reported for silk gels alone with ultrasonication.[16, 37] The band at 1164 cm^{-1} was assigned to the anti-symmetric stretching of C-O-C bridge, and 1064 cm^{-1} was assigned to the skeletal vibrations involving the C-O stretching, which shifted to 1071 cm^{-1} and 1075 cm^{-1} for SC2 and SC3, respectively. Moreover, the shifting of bands suggests the interaction between silk and chitosan. New interactions formed during sonication presumably leading to the shift of bands. The amide and carbonyl stretching absorption bands of chitosan and silk overlaps in the region 1598 cm^{-1} and 1655 cm^{-1}. The results from the ATR-FTIR indicate significant interactions between silk and chitosan.

2.7 Thermal analysis

The thermal properties of the sonication-induced silk and silk/chitosan scaffolds were determined by TGA and DSC (Figure 7). The thermal curves of SISF and silk/chitosan based hydrogels showed two step degradation behavior. The first small fraction of 4 to 7% weight loss was observed, which was mainly from the expulsion of bound and absorbed free water from the samples. The 2% weight

RSC Advances Accepted Manuscript

loss temperature of SISF was higher than that of its corresponding binary hydrogel. The derivative thermogram maximum increased with the addition of chitosan to the silk. The exception was the lower content of silk/chitosan hydrogel, SC1, which showed better thermal stability compared to higher content silk/chitosan gels in SC2 and SC3. This behavior could be attributed to the molecular interactions between silk and chitosan, when the concentration of chitosan was low. The residual weight in SISF was higher than SFS and also from silk/chitosan hydrogels.

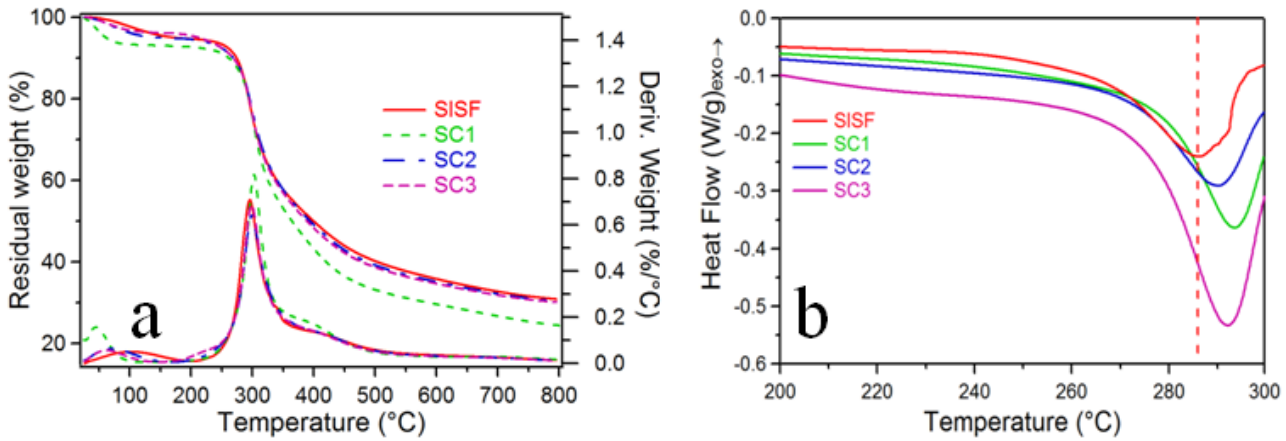

Figure 7. TGA spectra of sonication induced scaffolds (a) residual wt.% and derivative weight (%/°C) curves scanned at 10°C min^{-1} with a temperature range of 30–800°C under a 60 ml min^{-1} flow rate of nitrogen using a TA Q500 instrument, (b) DSC second heating curves of SISF and silk/chitosan at a scan rate of 10°C min^{-1} using a Mettler DSC822e module with STARe software under a nitrogen atmosphere at a 80 ml min^{-1} flow rate.

The DSC curves of SISF and silk/chitosan are shown in Figure 7b. The sonication induced silk/chitosan hydrogels showed an increase of degradation temperature in SC1. The DSC results indicated that there were some changes in the physical properties after interaction of the chitosan with silk. The increased temperature degradation stability was observed in case of the silk/chitosan hydrogels.

RSC Advances Accepted Manuscript

2.9. Cell culture

2.9.1. Cell viability, adhesion and proliferation

Cell viability was performed to assess potential cytotoxic cellular interactions by staining the cells inside the hydrogels and scaffolds with a cell-permeable fluorescent dye calcein AM. When live cells come in contact with calcein then the intact cell membranes accumulates calcein and hydrolyzes it by intracellular esterases to form a green-fluorescent product. Propidium iodide penetrates the membranes of dead cells and viable cells but PI is pumped out of the cells by viable cells. Whereas dead cells intercalates into the major groove of the DNA and produces highly fluorescent red adducts in non-viable cells. In order to assess cell-hydrogels and cell-scaffolds, MC3T3-E1 cells encapsulated in the sonicated silk and silk-chitosan hydrogels were examined by fluorescence microscopy after live/dead staining (Figure 11). All cells remained viable during the 15 days culture for the SISF (Figure 11a), SC1 (Figure 11b), SC2 (Figure 11c). In contrast, cells encapsulated in SC3 showed a reduced viability with more prominent propidium iodide staining.

In parallel, MC3T3-E1 cells were also seeded on the silk and silk-chitosan scaffolds and examined by fluorescence microscopy after live/dead staining (Figure 12). After 1 day, viable cells were spread and attached, irrespective of the silk-chitosan scaffold type (Figure 12 a-d). With increasing culture time, more area was covered by the cells. Thus the MC3T3-E1 cells adhered and proliferated and remained viable during the 15 day-culture period. These results further indicated that the sonication induced silk fibroin protein and silk fibroin protein-chitosan hydrogels and scaffolds were nontoxic and cell compatible.

RSC Advances Accepted Manuscript

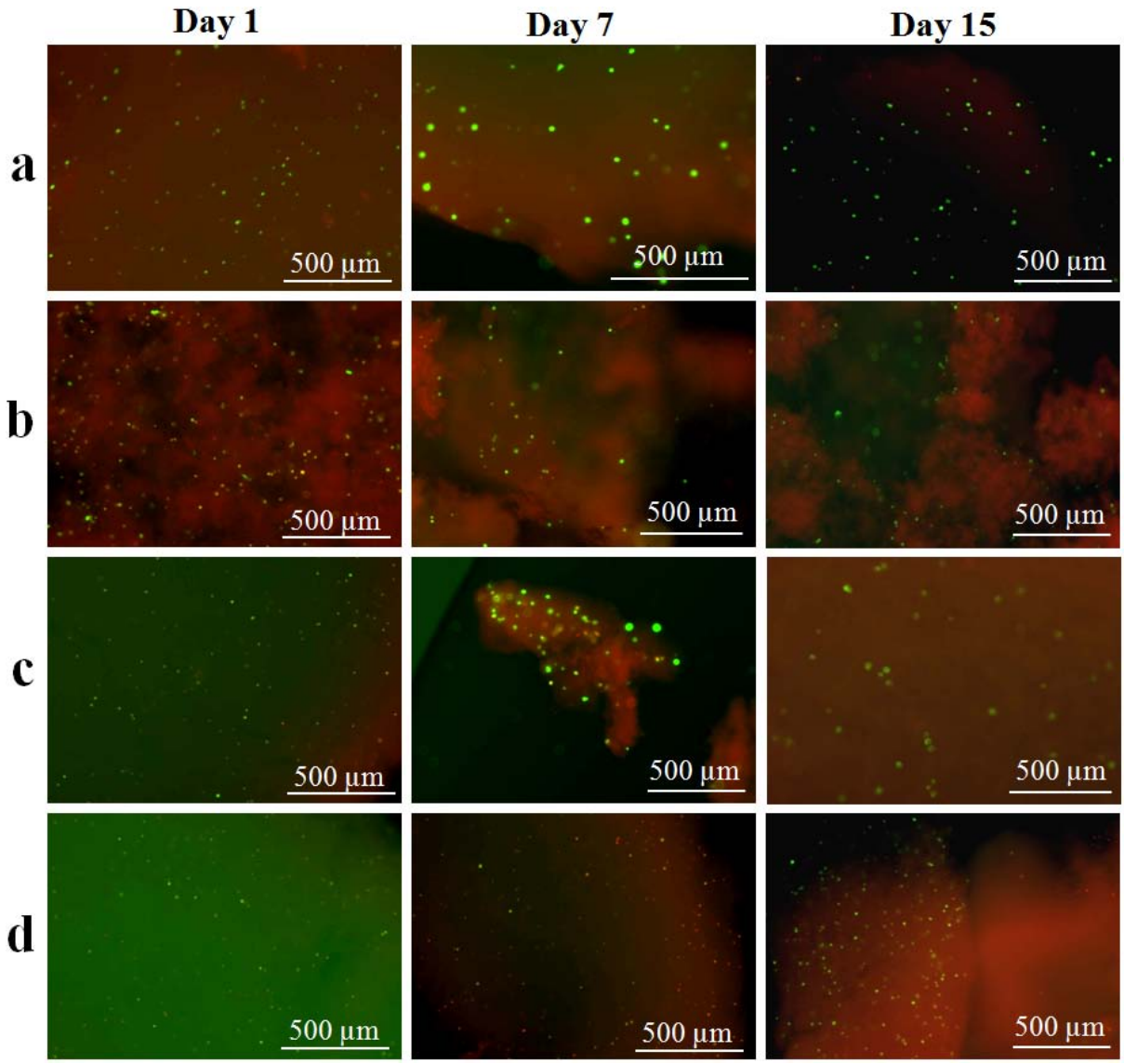

Figure 11. Fluorescence microscopy (CaAM/PI staining) viability of MC3T3 cells encapsulated in sonicated induced hydrogels for 1, 7 and 15 days (a) silk hydrogel, silk-chitosan hydrogels with (b) 10% of chitosan, (c) 25% of chitosan, (d) with 50% of chitosan.

RSC Advances Accepted Manuscript

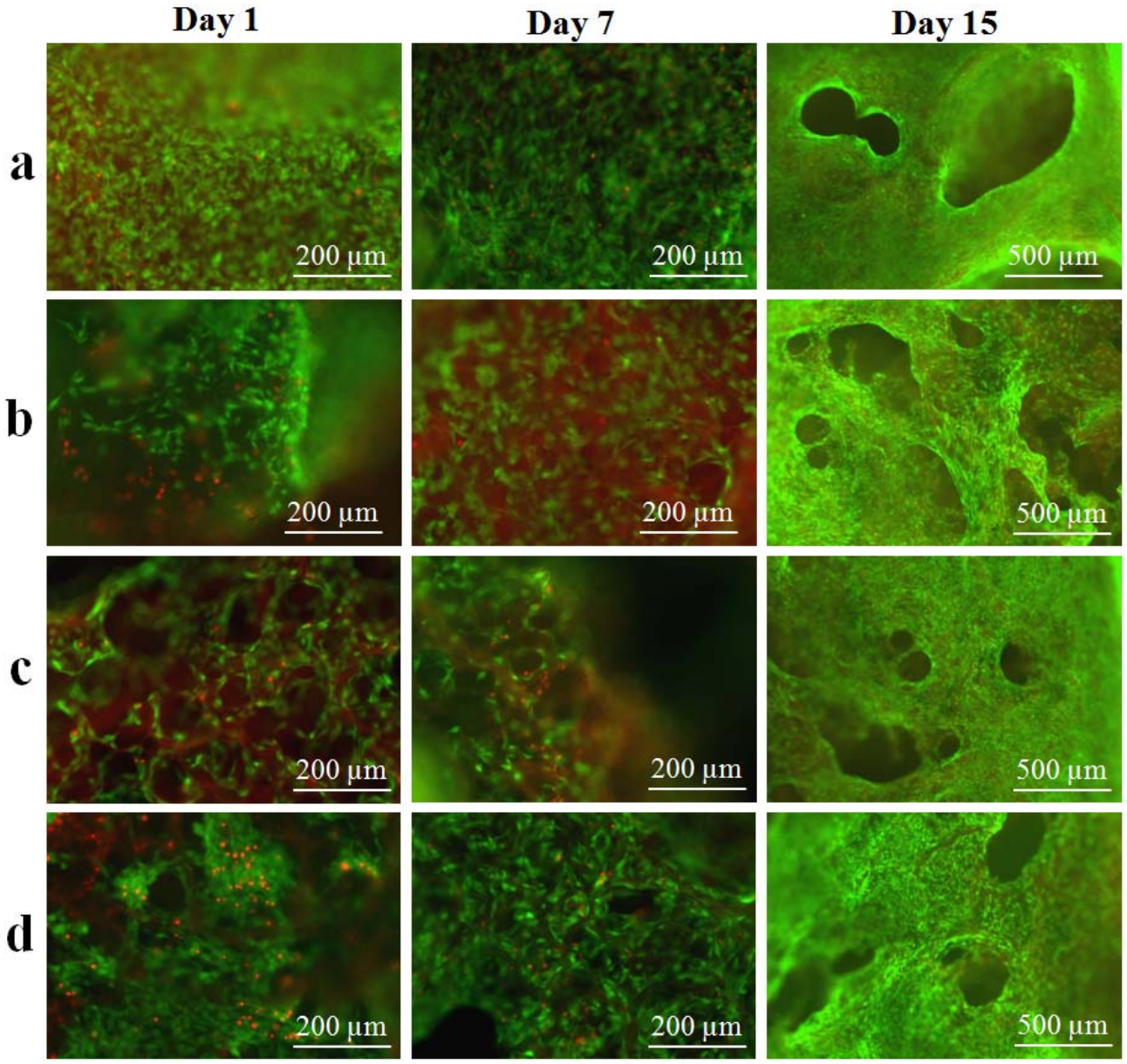

Figure 12. Viability of cells cultured on sonicated induced (a) silk scaffold (SISF), silk-chitosan scaffolds with (b) 10% of chitosan (CS1), (c) 25% of chitosan (CS2), (d) with 50% of chitosan (CS3). Fluorescence microscopy (CaAM/PI staining) of MC3T3 cells cultured on the scaffolds for 1, 7 and 15 days.

RSC Advances Accepted Manuscript

2.9.2. Histology of the cell encapsulated hydrogels and cell seeded scaffolds

To assess tissue morphology over time the sonicated hydrogels and scaffolds were harvested at various time points and processed for histological evaluation. The histology of sonication induced silk and silk-chitosan hydrogels where MC3T3 cells were encapsulated are shown in Figure 13. Cells encapsulated in the hydrogels retained their rounded shape throughout the culture period. In contrast to the silk hydrogels, where cells were encapsulated in a cavity, sections of silk/chitosan hydrogels embedded in paraffin had a different appearance (Fig. 13 b-d).

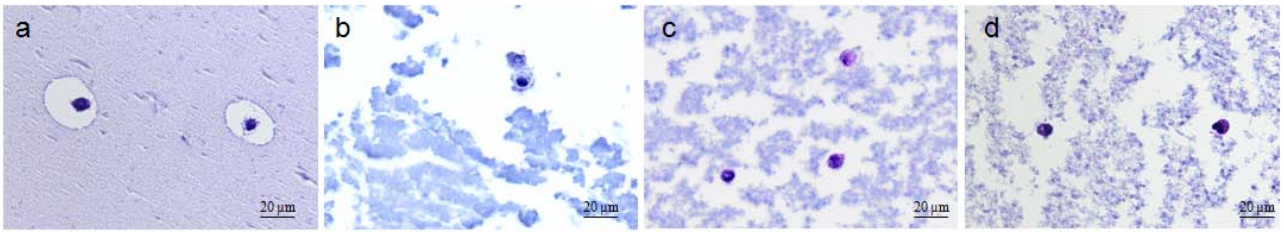

Figure 13. Histological analysis (H&E staining) of MC3T3 cells encapsulated in sonicated induced hydrogels for 15 days: (a) silk hydrogel (SISF), silk-chitosan hydrogels with (b) 10% of chitosan (CS1), (c) 25% of chitosan (CS2), (d) with 50% of chitosan (CS3).

The histology of sonication induced silk and silk-chitosan scaffolds seeded with MC3T3 cells is shown in Fig. 14. After 15 days in culture, the silk and silk-chitosan scaffolds were colonized by MC3T3 cells, irrespective of the scaffold type. The cells had an elongated shape, followed the contours of the scaffold and produced an extracellular matrix.

RSC Advances Accepted Manuscript

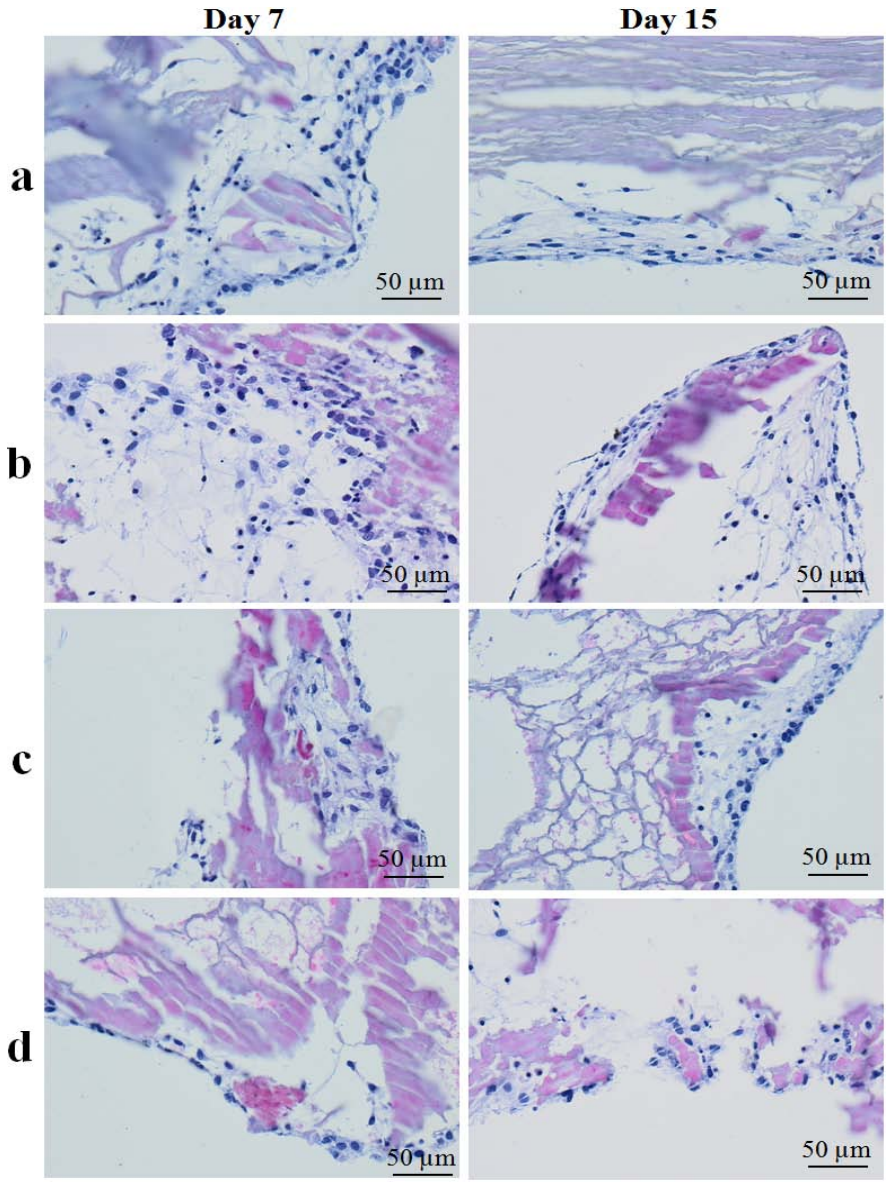

Figure 14. Histological analysis (H&E staining) of MC3T3 cells cultured on sonication induced 3D scaffolds for 7 and 15 days (a) silk scaffold (SISF), silk-chitosan scaffolds with (b) 10% of chitosan (CS1), (c) 25% of chitosan (CS2), (d) with 50% of chitosan (CS3).

3. Conclusions

In the present study an ultrasonication fabrication process was employed for the preparation of silk/chitosan biohybrid hydrogels and scaffolds. This strategy promoted the interaction between the two biopolymers with controllable, environmental friendly and non-toxic byproducts. Furthermore,

RSC Advances Accepted Manuscript

the present study elucidated that upon changing chitosan concentration the sonicated silk/chitosan scaffolds exhibited different architectures, with porous interconnected structures. The sonicated induced silk and silk-chitosan hydrogels/scaffolds were non-toxic and supported cell adhesion and colonization. The present study successfully developed a green technology towards conjugation of biopolymers for designing biohybrid silk-based biomaterials for tissue engineering and other therapeutic applications.

4. Experimental section

4.1 Materials

Cocoons from *Bombyx mori* silkworm were obtained from Tajima Shoji Co (Yokohama, Japan). Sodium carbonate (Na_2CO_3), lithium bromide (LiBr) and chitosan (medium molecular weight and degree of deacetylation (DD) = 75–85%) were purchased as reagent grade from Sigma–Aldrich or Fluka (St. Louis, MO) and used without further purification. Dialysis cassettes (Slide-a-Lyzer MWCO 3.5K) were purchased from Pierce biotechnology (Rockford, IL).

4.2 Preparation of aqueous silk solution

Aqueous silk solutions were prepared based on our published protocols.[3, 37, 40] Briefly, whole cocoons were cut into small pieces and were boiled in a 0.02M aqueous solution of Na_2CO_3. The remaining fibroin was rinsed thoroughly in deionized water and allowed to dry overnight. The dry fibroin was then dissolved in a 9.3 M aqueous solution of LiBr at 60°C for six hours. The LiBr was removed from the solution over the course of 48 hours by dialysis cassettes (Slide-a-Lyzer MWCO 3.5K, Pierce biotechnology, Rockford, IL) and remaining particulates were removed by centrifugation and syringe based micro-filtration (5 um pore size, Millipore Inc., Bedford, MA). This process enabled the production of 8–10 w/w % silk in water. Silk solutions with lower

RSC Advances Accepted Manuscript

concentrations were prepared by diluting the above solution with double distilled deionized water. The final silk concentration of the solution was monitored by drying 1 ml silk solution samples in a plastic petri dish at 60°C (American Scientific Products, Constant Temperature Oven, Model DK-42) and weighing the resulting dried films. All the samples were performed in triplicates.

4.3 Preparation of sonicated silk, silk/chitosan hydrogels and scaffolds

The silk fibroin protein solutions with concentrations of 8% (w/v) were prepared by diluting the original silk solution with water according to procedures described in the literature.[3, 37] Chitosan solution was prepared by dissolving 2 wt% chitosan in 1 wt% acetic acid. Then 8% silk fibroin protein was added to the chitosan solution to prepare different ratios of SF and chitosan (Table 3) and the solution was allowed to mix by magnetic stirrer for 15 min.

Table 3. Samples abbreviation with respect to sonication induced silk/chitosan gels and scaffolds.

Sonication induced sample	Abbreviation	Silk (%)	Chitosan (%)
Silk	SISF	100	—
Silk/low concentration of chitosan	SC1	90	10
Silk/medium concentration of chitosan	SC2	75	25
Silk/high concentration of chitosan	SC3	50	50

The blend solutions, 4 ml, were poured into 15 ml-Falcon tubes and sonicated for 2 minutes with a Branson 450 Sonifier (Branson Ultrasonics Co., Danbury, CT), which consisted of the Model 450 power supply, converter, externally threaded disruptor horn and 1/8" (3.175 mm) diameter-tapered microtip following our previously reported procedures.[16] Immediately after sonication the white colored solution was transferred into 24 well plate molds and considered a hydrogel. The hydrogels were kept overnight at -4°C to assess swelling and water content. The remaining hydrogels samples were transferred to a -20°C freezer for 24 hrs, followed by lyophilization for 48 hrs and considered

RSC Advances Accepted Manuscript

as scaffold. The dry samples were removed from the molds and stored in airtight 24 well plates with vacuum air bags at –4°C to avoid changes over time prior to analysis.

4.4 Scanning electron microscopy (SEM)

The lyophilized silk/chitosan samples were mounted on sample holder fixed with double-sided adhesive tape. The samples were sputter coated with gold prior to SEM analysis. The morphologies of samples were observed using a JEOL scanning electron microscope (SEM) (JSM-5600LV, Tokyo, Japan) at the required magnification and with an accelerating voltage of 12kV.

4.5 Wide angle X-ray scattering (WAXS)

The lyophilized silk/chitosan samples were grinded in a ceramic mortar to obtain powder of respective samples. WAXS diffraction patterns were performed on powdered lyophilized silk/chitosan samples at room temperature with a Kristalloflex 810 diffractometer (SIEMENS, Karlsruhe, Germany) using a Cu Kα (λ=1.5406 Å) as X-ray source. Scans were run in the high angle region $5° < 2\theta < 65°$ at a scan rate of 0.040°/min and a dwell time of 2s.

4.6 Attenuated Total Reflectance FTIR (ATR-FTIR)

The lyophilized silk/chitosan samples were grinded in a ceramic mortar to obtained powder of respective samples. ATR-FTIR was performed on powdered lyophilized silk/chitosan samples with JASCO FTIR- 6200 (Tokyo, Japan) equipped with a MIRacle attenuated total reflection (ATR) Crystal Ge (IR penetration 0.66 mm) cell in reflection mode and absorbance of spectra were at 32 scans coded with 4 cm^{-1} resolution in the region 5000-700 cm^{-1}.

RSC Advances Accepted Manuscript

4.7 Deswelling kinetics

The deswelling kinetics of samples was measured by water weight loss over time under isothermal conditions at 37°C. The sonication induced hydrogels were thoroughly washed with distilled water and immersed in a distilled water bath at 37°C for 5 hrs to obtain samples fully equilibrated in the swollen state. The swollen hydrogel samples were removed from the distilled water bath and subjected to deswelling kinetic assessments by isothermal thermogravimetric (TGA) treatment at 37°C in a TA Q500-thermobalance (TA Instruments, Milan, Italy). The weight loss of 10-15 mg specimens was tracked over 4 hrs under a nitrogen atmosphere at a flow rate of 60 mL·min^{-1}.

4.8 State of water

The state of water of samples were investigated by differential scanning calorimetry (DSC). DSC evaluations were carried out on a Mettler DSC822e module (Mettler Toledo, Milan, Italy) controlled by STARe software under a nitrogen atmosphere at 80 mL·min^{-1} flow rate. Equilibrated swelled state of hydrogel samples of 3 to 5 mg were weighed in 40 µL aluminum pans and an empty pan was used as reference. The experiments were performed with 5 samples each. DSC temperature calibration was performed using indium standards. Measurements were performed according to the following protocol.[39] Cooling scan from 25°C to –70°C at 10° C·min^{-1} and isotherm of 5 min at the ending temperature; and

1. Heating scan from –70°C to 50°C at 10° C·min^{-1}.

The equations used to calculate these states of water are the following:

$$w_f = Q_w / \Delta H_w \quad (1)$$

$$w_{nf} = w_t - w_f \quad (2)$$

where, w_f, w_{nf} and w_t are the weight of freezable, non-freezable and total water in swelled membranes, respectively, and Q_w is the measured heat of crystallization in Joules andΔHw is the

RSC Advances Accepted Manuscript

enthalpy of the ice-water transition obtained from pristine water, which is 393 $J \cdot g^{-1}$ measured on cooling.

4.9 Thermogravimetric analysis (TGA)

The lyophilized silk/chitosan samples were grinded in a ceramic mortar to obtained powder of respective samples. TGA experiments were performed on powdered lyophilized silk/chitosan samples in the TA Instruments Series TA Q500 (TA Instruments, Milan, Italy) with Thermogravimetric Analyzer Software. Sample weights were between 9-13 mg and were scanned at $10°C \cdot min^{-1}$. The temperature range was 30°C to 900°C under a 60 $mL \cdot min^{-1}$ flow rate of nitrogen.

4.10 Differential scanning calorimetry (DSC)

Thermodynamic parameters of the samples were assessed on a Mettler DSC822e module (Mettler Toledo, Milan, Italy) controlled by the STARe software under a nitrogen atmosphere at 80 $mL \cdot min^{-1}$ flow rate with three scans. Samples of 3–9 mg were weighed in standard 40 μL aluminum pans and an empty pan was used as reference. Measurements were performed in accordance with ASTM D 3418 methods under a nitrogen flow rate of 80 $mL \cdot min^{-1}$ according to the following protocols:

1. First heating scan from -20°C to 180°C at $10°C \cdot min^{-1}$ and 3 min of isothermal conditions at the end;
2. First cooling scan from 180°C to -20°C at $-10°C \cdot min^{-1}$ and 3 min of isothermal conditions at the end
3. Second heating scan from -20°C to 300°C at 10 $°C \cdot min^{-1}$.

RSC Advances Accepted Manuscript

4.11 Cell culture

4. 11. 1 Cell encapsulation and cell seeding

MC3T3-E1 cells (mouse calvaria preosteoblast cells, subclone 14, ATCC) were cultured in α-MEM L-glutamax (Gibco Invitrogen) supplemented with 10% fetal bovine serum (FBS, Gibco Invitrogen) and 0.5 vol% penicillin-streptomycin (10,000 U/ml-10,000 µg/ml, Gibco Invitrogen). Cells were cultured at 37°C in a humidified atmosphere of 5% CO_2.

Cell encapsulation in sonicated hydrogels

Silk solution of 8 % (w/v) and chitosan solution of 2% were sterilized by keeping in microwave oven two times for 2 minutes. The hot silk and chitosan solutions were kept under the laminar flow hood for cooling down to room temperature. An aliquot of 1 mL of silk and the different ratio silk and chitosan solution were pipetted in to 1.5-mL Eppendorf and mixed well by pipetting before exposing to sonication. The sonication was performed as explained before, and within 1 minute 200 µL of the MC3T3-E1 cell suspension was added and mixed with the sonicated silk/chitosan solution to reach a final concentration of 0.5x 10^6 cells/mL. An aliquot of 600 µL of the gel and cell suspension mixtures was quickly pipetted into 12-well cell culture plates, with a total of five samples prepared for each sample group. The hydrogels were then cultured in 1 mL of growth medium. All plates were incubated at 37°C and 5% CO_2. For microscopy imaging, the cell encapsulated gels were punched out and images were taken at desired time points.

Cell seeding on scaffolds

The silk and silk-chitosan scaffolds (diameter 6 mm, height 5 mm) were sterilized by ethylene oxide cold cycle (Maria Middelares Hospital, Ghent, Belgium). The scaffolds were placed into 24-well tissue culture dishes and seeded at a density of 0.5x10^6 cells/40 µl/scaffold and were allowed to adhere for 15 minutes. Culture medium (1 ml) was added to each well and the seeded scaffolds were cultured for 15 days (5% CO_2/95% air, 37°C).

RSC Advances Accepted Manuscript

4. 11. 2 Characterization of cell/hydrogel and cell/scaffold constructs

Cell viability, adhesion, proliferation and colonization were evaluated at different time points with the following analyses.

4.11.2.1. Fluorescence microscopy

To visualize cell viability, adhesion or colonization, cell-hydrogel and cell-scaffold constructs were evaluated using fluorescence microscopy after performing live/dead staining. After rinsing with PBS, the supernatant was replaced by 1 ml PBS solution supplemented with 2 µl (1 mg/ml) calcein AM (Anaspec, USA) and 2 µl propidium iodide (PI) (1 mg/ml) (Sigma-Aldrich). Cultures were incubated for 10 minutes at room temperature, washed twice with PBS solution and evaluated by fluorescence microscopy (Olympus inverted Research System Microscope, type U-RFL-T, XCellence Pro software, Olympus, Belgium). Evaluations were done post-seeding at day 1, 7 and 15 days.

4.11.2.4. Histology

Cell/hydrogel and cell/scaffold constructs were rinsed with PBS solution, fixed with 4% phosphate (10 mM) buffered formaldehyde (pH 6.9) (4°C, 24 h), dehydrated in a graded alcohol series and embedded in paraffin. The scaffolds were sectioned (5-7 µm), stained with hematoxylin & eosin (H&E) and mounted with mounting medium (Cat.No. 4111E, Richard-Allan Scientific).

4.12 Statistical analysis

Statistical significance between multiple groups was calculated by a one-way analysis of variance (ANOVA). The Student's t test was used for the statistical significance of differences between average values of two independent groups at 95% confidence ($p < 0.05$).

RSC Advances Accepted Manuscript

Notes.

The authors declare no competing financial interest.

5. Acknowledgements

Authors would like to thank Carmen Preda and Guokui Qin for their technical help. The authors would also like to thank Bimolecular Sciences School, University of Pisa, Italy and the NIH (P41 EB002520) for financial support.

6. References

1. D. N. Rockwood, R. C. Preda, T. Yucel, X. Wang, M. L. Lovett and D. L. Kaplan, *Nat. Protocols*, 2011, **6**, 1612-1631.
2. C. Vepari and D. L. Kaplan, *Progress in Polymer Science*, 2007, **32**, 991-1007.
3. S. K. Samal, M. Dash, F. Chiellini, D. L. Kaplan and E. Chiellini, *Acta Biomaterialia*, 2013, **9**, 8192-8199.
4. M. Fedel, T. Endogan, N. Hasirci, D. Maniglio, A. Morelli, F. Chiellini and A. Motta, *Journal of Bioactive and Compatible Polymers*, 2012.
5. X. Zhang, M. R. Reagan and D. L. Kaplan, *Advanced Drug Delivery Reviews*, 2009, **61**, 988-1006.
6. A. Motta, D. Maniglio, C. Migliaresi, H.-J. Kim, X. Wan, X. Hu and D. L. Kaplan, *Journal of Biomaterials Science, Polymer Edition*, 2009, **20**, 1875-1897.
7. Y. Wang, U.-J. Kim, D. J. Blasioli, H.-J. Kim and D. L. Kaplan, *Biomaterials*, 2005, **26**, 7082-7094.
8. X. H. Zou, Y. L. Zhi, X. Chen, H. M. Jin, L. L. Wang, Y. Z. Jiang, Z. Yin and H. W. Ouyang, *Biomaterials*, 2010, **31**, 4872-4879.
9. P. He, K. S. Ng, S. L. Toh and J. C. H. Goh, *Biomacromolecules*, 2012, **13**, 2692-2703.
10. H. Liu, X. Ding, Y. Bi, X. Gong, X. Li, G. Zhou and Y. Fan, *Macromolecular Bioscience*, 2013, **13**, 755-766.

RSC Advances Accepted Manuscript

11. G. H. Altman, F. Diaz, C. Jakuba, T. Calabro, R. L. Horan, J. Chen, H. Lu, J. Richmond and D. L. Kaplan, *Biomaterials*, 2003, **24**, 401-416.
12. Y. Wang, H.-J. Kim, G. Vunjak-Novakovic and D. L. Kaplan, *Biomaterials*, 2006, **27**, 6064-6082.
13. A. Vasconcelos, G. Freddi and A. Cavaco-Paulo, *Biomacromolecules*, 2008, **9**, 1299-1305.
14. A. Motta, L. Fambri and C. Migliaresi, *Macromolecular Chemistry and Physics*, 2002, **203**, 1658-1665.
15. T. Asakura, R. Sugino, T. Okumura and Y. Nakazawa, *Protein Science*, 2002, **11**, 1873-1877.
16. X. Wang, J. A. Kluge, G. G. Leisk and D. L. Kaplan, *Biomaterials*, 2008, **29**, 1054-1064.
17. T. Yucel, P. Cebe and D. L. Kaplan, *Biophysical Journal*, 2009, **97**, 2044-2050.
18. M. Dash, F. Chiellini, R. M. Ottenbrite and E. Chiellini, *Progress in Polymer Science*, 2011, **36**, 981-1014.
19. S. K. Samal, M. Dash, S. Van Vlierberghe, D. L. Kaplan, E. Chiellini, C. van Blitterswijk, L. Moroni and P. Dubruel, *Chemical Society Reviews*, 2012, **41**, 7147-7194.
20. C. K. S. Pillai, W. Paul and C. P. Sharma, *Progress in Polymer Science*, 2009, **34**, 641-678.
21. D. X. Oh and D. S. Hwang, *Biotechnology Progress*, 2013, **29**, 505-512.
22. S. Kumar and J. Koh, *International Journal of Molecular Sciences*, 2012, **13**, 6102-6116.
23. J. G. Fernandez and D. E. Ingber, *Advanced Materials*, 2012, **24**, 480-484.
24. S. S. Silva, A. Motta, M. r. T. Rodrigues, A. F. M. Pinheiro, M. E. Gomes, J. o. F. Mano, R. L. Reis and C. Migliaresi, *Biomacromolecules*, 2008, **9**, 2764-2774.
25. A. Sionkowska and A. Płanecka, *Journal of Molecular Liquids*, 2013, **178**, 5-14.
26. X.-X. Xia, Q. Xu, X. Hu, G. Qin and D. L. Kaplan, *Biomacromolecules*, 2011, **12**, 3844-3850.
27. A. M. Altman, V. Gupta, C. N. Ríos, E. U. Alt and A. B. Mathur, *Acta Biomaterialia*, 2010, **6**, 1388-1397.
28. A. M. Altman, Y. Yan, N. Matthias, X. Bai, C. Rios, A. B. Mathur, Y.-H. Song and E. U. Alt, *STEM CELLS*, 2009, **27**, 250-258.
29. H. K. Makadia and S. J. Siegel, *Polymers-Basel*, 2011, **3**, 1377-1397.
30. K. Grodowska and A. Parczewski, *Acta Pol Pharm*, 2010, **67**, 3-12.

RSC Advances Accepted Manuscript

31. P. J. Ginty, M. J. Whitaker, K. M. Shakesheff and S. M. Howdle, *Materials Today*, 2005, **8**, 42-48.

32. R. Falk and T. Randolph, *Pharm Res*, 1998, **15**, 1233-1237.

33. X. Wang, W. Li and V. Kumar, *Biomaterials*, 2006, **27**, 1924-1929.

34. G. Cravotto and P. Cintas, *Chemical Science*, 2012, **3**, 295-307.

35. K. S. Suslick and G. J. Price, *Annual Review of Materials Science*, 1999, **29**, 295-326.

36. J. M. J. Paulusse and R. P. Sijbesma, *Journal of Polymer Science Part A: Polymer Chemistry*, 2006, **44**, 5445-5453.

37. S. K. Samal, D. L. Kaplan and E. Chiellini, *Macromolecular Materials and Engineering*, 2013, n/a-n/a.

38. H. Elhendawi, R. M. Felfel, B. M. Abd El-Hady and F. M. Reicha, *ISRN Biomaterials*, 2014, **2014**, 8.

39. S. Samal, E. Fernandes, F. Chiellini and E. Chiellini, *J Therm Anal Calorim*, 2009, **97**, 859-864.

40. S. Sofia, M. B. McCarthy, G. Gronowicz and D. L. Kaplan, *Journal of Biomedical Materials Research*, 2001, **54**, 139-148.

RSC Advances Accepted Manuscript

Table of contents

A green technology approach towards conjugation of biopolymers for designing biohybrid silk/chitosan based biomaterials for therapeutic applications.

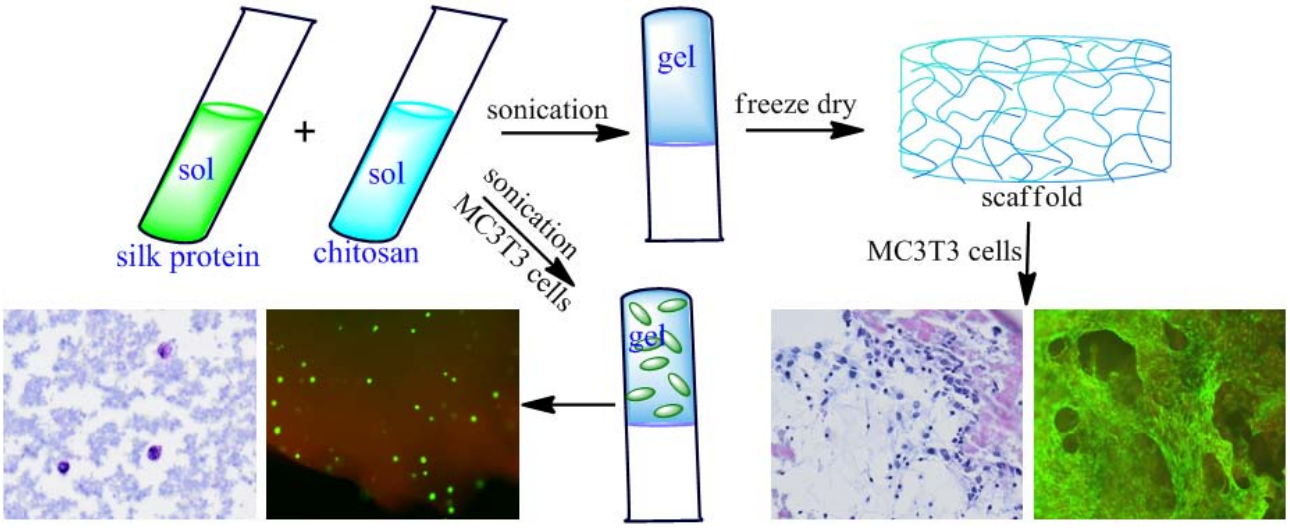

RSC Advances Accepted Manuscript